*Inorg. Chem.* **2004**, *43*, 6015–6023


# Synthesis, Structure, Magnetism, and Spectroscopic Properties of Heterobinuclear Copper(II)–Zinc(II) Complexes and Their Copper(II)–Copper(II) Analogues in Asymmetric Ligand Environments

**Dipesh Ghosh,[†] Nabanita Kundu,[†] Goutam Maity,[†] Ki-Young Choi,[‡] Andrea Caneschi,[§] Akira Endo,[||] and Muktimoy Chaudhury*,[†]**

*Department of Inorganic Chemistry, Indian Association for the Cultivation of Science, Kolkata 700 032, India, Department of Chemistry Education, Kongju National University, Kongju 314-701, South Korea, Department of Chemistry, Polo Scientifico of the University of Florence, 50019 Sesto Fiorentino, Firenze, Italy, and Department of Chemistry, Faculty of Science and Technology, Sophia University, 7-1 Kioi-cho, Chiyoda-ku, Tokyo 102-8554, Japan*

Received April 29, 2004

Heterobinuclear copper(II)–zinc(II) complexes and their homobinuclear dicopper(II) counterparts (**1**–**4**) of two asymmetric ligands ($H_2L^1$ and $H_2L^2$), based on 2-aminocyclopent-1-ene-1-dithiocarboxylate, are reported. The ligands are capable of providing both donor set and coordination number asymmetry in tandem. Metal centers in these complexes are connected by a $\mu$-alkoxo and a bridging pyrazolate moiety, as confirmed by X-ray structure analyses of **1**, **3**, and **4**. The Cu(1) site in the dicopper complex (**1**) is square planar and so are the copper sites in the Cu–Zn complexes **3** and **4**. The pentacoordinated Zn sites in the latter complexes have distorted TBP geometry ($\tau = 0.74$), while the corresponding Cu site in **1** has a highly distorted square pyramidal structure ($\tau = 0.54$). The Cu···Zn separations in **3** and **4** are 3.3782 and 3.3403 Å, respectively, while the Cu···Cu distance in **1** is 3.3687 Å. The dicopper complexes are EPR silent at 77 K, in which the copper(II) centers are coupled by strong antiferromagnetic coupling ($J$ = ca. $-290$ cm$^{-1}$) as confirmed by variable-temperature (4–300 K) magnetic measurements. These compounds (**1** and **2**) undergo two one-electron reductions and a single step two-electron oxidation at ca. $-0.26$, $-1.40$, and 1.0 V vs Ag/AgCl reference, respectively, as indicated by cyclic and differential pulse voltammetry done at subambient temperatures. EPR spectra of **3** and **4** display axial anisotropy at 77 K with the $g_\perp$ region being split into multiple lines due to N-superhyperfine coupling ($A_N = 15.3 \times 10^{-4}$ cm$^{-1}$). The observed trend in the spin-Hamiltonian parameters, $g_{||} > g_\perp > 2.04$ and $|A_\perp| \ll |A_{||}| \approx (120–150) \times 10^{-4}$ cm$^{-1}$, indicates a $d_{x^2-y^2}$-based ground state with tetragonal site symmetry for the Cu(II) center in these molecules.

## Introduction

Binuclear centers containing transition elements are ubiquitous in metalloproteins.[1] Some representative examples of structurally characterized homo- and heterobinuclear active sites are those in non-heme manganese catalase [Mn,Mn],[2] urease [Ni,Ni],[3] alkaline phosphatase [Zn,Zn],[4] purple acid phosphatase [Fe,Zn],[5] human protein phosphatase 1 [Mn,Fe],[6] and bovine erythrocyte superoxide dismutase (SOD) [Cu,Zn];[7] in each case the metal centers have asymmetric ligand environments.[8] For example in SOD, the copper

* Author to whom correspondence should be addressed. E-mail: icmc@mahendra.iacs.res.in.
[†] Indian Association for the Cultivation of Science.
[‡] Kongju National University.
[§] University of Florence.
[||] Sophia University.

(1) (a) *Bioinorganic Chemistry of Copper*; Karlin, K. D., Tylekar, Z., Eds; Chapman & Hall: New York, 1993. (b) Que, L., Jr.; True, A. E. *Prog. Inorg. Chem.* **1990**, *38*, 97. (c) Solomon, E. I.; Baldwin, M. J.; Lowery, M. D. *Chem. Rev.* **1992**, *92*, 521. (d) Solomon, E. I. In *Metal Clusters in Proteins*; Que, L., Jr., Ed.; ACS Symposium Series 372; American Chemical Society: Washington, DC, 1988; pp 116−150.
(2) Barynin, V. V.; Vagin, A. A.; Melik-Adamyan, V. R.; Grebenko, A. I.; Khangulov, S. V.; Popov, A. N.; Andrionova, M. E.; Vainshtein, B. K. *Dokl. Akad. Nauk. SSR* **1986**, *288*, 877.
(3) Jabri, E.; Carr, M. B.; Hausinger, R. P.; Karplus, P. A. *Science* **1995**, *268*, 998.
(4) Kim, E. E.; Wyckoff, H. W. *J. Mol. Biol.* **1991**, *218*, 449.
(5) Sträter, N.; Klabunde, T.; Tucker, P.; Witzel, H.; Krebs, B. *Science* **1995**, *268*, 1489.
(6) Egloff, M.-P.; Cohen, P. T. W.; Reinemer, P.; Barford, D. *J. Mol. Biol.* **1995**, *254*, 942.

10.1021/ic049449+ CCC: $27.50 
Published on Web 08/19/2004

center has a distorted square-pyramidal geometry involving four imidazole groups, one of which is deprotonated and acts as a bridge to the zinc center which has an approximate tetrahedral geometry. The Cu····Zn distance is 5.4 Å. The latter enzyme is known to play a significant role in biology by protecting organisms from the cytotoxic effects of superoxide ion, $O_2^-$, by catalyzing its dismutation to dioxygen and hydrogen peroxide through a rapid two-step cyclical process (eqs 1 and 2) involving alternative reduction and oxidation of the active-site copper(II) center.[9,10]

$$O_2^- + ECu^{II} \rightleftharpoons O_2 + ECu^{I} \quad (1)$$

$$O_2^- + ECu^{I} + 2H^+ \rightleftharpoons H_2O_2 + ECu^{II} \quad (2)$$

These observations set an objective to design and synthesize binuclear imidazole-bridged Cu/Zn compounds as biomimetic models to understand the role(s) of these metal ions in the overall functioning of SOD. Only a few imidazole-bridged binuclear Cu/Zn compounds have been reported thus far,[11−17] because of the inherent difficulties in their preparation. Unfortunately, all of these complexes, unlike their natural counterparts, have symmetrical ligand environments around the metal centers and thus fail to be a more realistic structural model for the SOD active site.[7,8,18]

For quite sometime, we have an ongoing project involving the coordination chemistry of 2-aminocyclopent-1-ene-1-dithiocarboxylate-based ligands with diverse transition metal ions.[19−23] Very recently, we reported[19] nickel(II) complexes of a binucleating "end off" ligand,[24] viz. methyl 2-(2-bis-((3,5-dimethylpyrazol-1-yl-methyl)amino)-2-hydroxypropylamino)cyclopent-1-ene-1-dithiocarboxylate ($H_2L^1$), capable of providing both donor set and coordination number asymmetry in tandem. The perception that the binuclear active sites of many metalloenzymes including SOD situate their metal centers in chemically distinct environments has motivated us to synthesize binuclear copper(II)−zinc(II) compounds in unsymmetrical acyclic ligand environments. Herein, we report the syntheses of pyrazolato-bridged binuclear copper(II)−zinc(II) complexes along with their dicopper(II) analogues using the aforesaid and a closely similar asymmetric ligand ($H_2L^2$). X-ray crystallography, EPR and electronic spectroscopy, and variable-temperature (4−300 K) magnetic susceptibility measurements have been carried out to characterize these compounds. Their redox properties have been investigated by cyclic and differential pulse voltammetry.

## Experimental Section

**Materials.** The ligand $H_2L^1$ was prepared as described elsewhere.[19] For the second ligand, viz. methyl 2-(2-bis((pyrazol-1-yl-methyl)amino)-2-hydroxypropylamino)cyclopent-1-ene-1-dithiocarboxylate ($H_2L^2$), an identical procedure was used except that 1-hydroxymethylpyrazole[25] was used instead of 1-(hydroxymethyl)-3,5-dimethylpyrazole. $[Cu(CH_3CN)_4]ClO_4$ was prepared by following a reported method.[26] Solvents were reagent grade, dried by standard methods,[27] and distilled under nitrogen prior to their use. All other chemicals were commercially available and used as received.

**Syntheses. $[Cu_2L^m(\mu\text{-pz})]BPh_4$ (1).**[28] To an acetonitrile solution (10 mL) of $H_2L^1$ (0.23 g, 0.5 mmol) was added 2 equiv of $[Cu(CH_3CN)_4]ClO_4$ (0.33 g, 1 mmol) dissolved in acetonitrile (10 mL), with stirring under $N_2$. After 10 min, 1 equiv of pyrazole (35 mg, 0.5 mmol) in acetonitrile (5 mL) was added, followed by triethylamine (0.5 mmol). The resulting mixture was stirred for 0.5 h to get a red brown solution. It was then exposed to atmospheric oxygen and stirred further for ca. 2 h. The dark brown solution obtained at this stage was filtered, and the filtrate volume was reduced to ca. 10 mL, combined with $NaBPh_4$ (0.17 g, 0.5 mmol), and allowed to stand at 0 °C for an overnight period to get a brown microcrystalline solid. The product was collected by filtration and finally recrystallized from acetonitrile. Yield: 0.18 g (38%). Anal. Calcd for $C_{47}H_{51}N_8S_2OCu_2B$: C, 59.69; H, 5.40; N, 11.85. Found: C, 59.89; H, 5.49; N, 11.78. IR (KBr pellet), $cm^{-1}$: $\nu$(C−C), 1580 m; $\nu$(C−N)/pyrazole ring, 1556 m; $\nu$(C−C + C−N), 1469 s, 1421 m; $\nu(BPh_4^-)$, 737 and 705 s. MS data: $m/z$ 625.0, $[M - BPh_4]^+$. $\mu_{eff}$: 1.93 $\mu_B$ at 25 °C.

**$[Cu_2L^2(\mu\text{-pz})]ClO_4$ (2).** This compound was prepared in the same manner as described above for **1** using $H_2L^2$ as the ligand. The compound was isolated as the perchlorate salt. Yield: 0.19 g (56%). Anal. Calcd for $C_{21}H_{27}N_8S_2O_5Cu_2Cl$: C, 36.13; H, 3.87; N, 16.05. Found: C, 36.29; H, 3.89; N, 16.35. IR (KBr pellet), $cm^{-1}$:


(7) (a) Tainer, J. A.; Getzoff, E. D.; Beem, K. M.; Richardson, J. S.; Richardson, D. C. *J. Mol. Biol*. **1982**, *160*, 181. (b) Tainer, J. A.; Getzoff, E. D.; Richardson, J. S.; Richardson, D. C. *Nature* **1983**, *306*, 284.
(8) Belle, C.; Pierre, J.-L. *Eur. J. Inorg. Chem*. **2003**, 4137.
(9) (a) McCord, J. M.; Fridovich, I. *J. Biol. Chem*. **1969**, *244*, 6049. (b) Fridovich, I. *Annu. Rev. Biochem*. **1995**, *64*, 97.
(10) Klug-Roth, D.; Fridovich, I.; Rabani, J. *J. Am. Chem. Soc*. **1973**, *95*, 2786. (b) Rotilio, G.; Bray, R. C.; Fielden, E. M. *Biochim. Biophys. Acta* **1972**, *268*, 605.
(11) Sato, M.; Nagae, S.; Uehara, M.; Nakaya, J. *J. Chem. Soc., Chem. Commun*. **1984**, 1661.
(12) Lu, Q.; Luo, Q. H.; Dai, A. B.; Zhou, Z. Y.; Hu, G. Z. *J. Chem. Soc., Chem. Commun*. **1990**, 1429.
(13) Zongwan, M.; Dong, C.; Wenxia, T.; Kaibei, Y.; Li, L. *Polyhedron* **1992**, *11*, 191.
(14) Pierre, J.-L.; Chautemps, P.; Refaif, S.; Beguin, C.; Marzouki, A. E.; Serratrice, G.; Saint-Aman, E.; Rey, P. *J. Am. Chem. Soc*. **1995**, *117*, 1965.
(15) Mao, Z.-W.; Chen, M.-Q.; Tan, X.-S.; Liu, J.; Tang, W.-X. *Inorg. Chem*. **1995**, *34*, 2889.
(16) (a) Ohtsu, H.; Itoh, S.; Nagatomo, S.; Kitagawa, T.; Ogo, S.; Watanabe, Y.; Fukuzumi, S. *J. Chem. Soc., Chem. Commun*. **2000**, 1051. (b) Ohtsu, H.; Shimazaki, Y.; Odani, A.; Yamauchi, O.; Mori, W.; Itoh, S.; Fukuzumi, S. *J. Am. Chem. Soc*. **2000**, *122*, 5733.
(17) (a) Li, S.; Li, D.; Yang, D.; Li, Y.; Huang, J.; Yu, K.; Tang, W. *Chem. Commun*. **2003**, 880. (b) Li, D.; Li, S.; Yang, D.; Yu, J.; Huang, J.; Li, Y.; Tang, W. *Inorg. Chem*. **2003**, *42*, 6071.
(18) (a) Fenton, D. E. *Chem. Soc. Rev*. **1999**, *28*, 159. (b) Sorrell, T. N. *Tetrahedron* **1989**, *45*, 3.
(19) Ghosh, D.; Mukhopadhyay, S.; Samanta, S.; Choi, K.-Y.; Endo, A.; Chaudhury, M. *Inorg. Chem*. **2003**, *42*, 7189.
(20) Bhattacharyya, S.; Mukhopadhyay, S.; Samanta, S.; Weakley, T. J. R.; Chaudhury, M. *Inorg. Chem*. **2002**, *41*, 2433.
(21) Bhattacharyya, S.; Weakley, T. J. R.; Chaudhury, M. *Inorg. Chem*. **1999**, *38*, 633.
(22) Bhattacharyya, S.; Weakley, T. J. R.; Chaudhury, M. *Inorg. Chem*. **1999**, *38*, 5453.
(23) Bhattacharyya, S.; Kumar, S. B.; Dutta, S. K.; Tiekink, E. R. T.; Chaudhury, M. *Inorg. Chem*. **1996**, *35*, 1967.
(24) Crane, J. D.; Fenton, D. E.; Latour, J. M.; Smith, A. J. *J. Chem. Soc., Dalton Trans*. **1991**, 2979.
(25) Driessen, W. L. *Recl. Trav. Chim. Pays-Bas* **1982**, *101*, 441.
(26) Hemmerich, P.; Sigwart, C. *Experientia* **1963**, *19*, 488.
(27) Perrin, D. D.; Armarego, W. L. F.; Perrin, D. R. *Purification of Laboratory Chemicals*, 2nd ed.; Pergamon: Oxford, England, 1980.

(28) The original $H_2L^1$ ligand undergoes interesting modification during the progress of the reaction. The changed form of the ligand is denoted by $(L^m)^{2-}$.

**Table 1.** Crystal Data for Complexes **1**, **3**, and **4**

| | **1** | **3** | **4** |
|---|---|---|---|
| composn | $C_{47}H_{51}BCu_2N_8OS_2$ | $C_{47}H_{51}BCuN_8OS_2Zn$ | $C_{23}H_{30}ClCuN_9O_5S_2Zn$ |
| fw | 945.97 | 947.80 | 741.04 |
| cryst system | monoclinic | monoclinic | monoclinic |
| space group | $P2_1/n$ | $P2_1/n$ | $P2_1/c$ |
| *a*, Å | 18.988(3) | 18.882(3) | 12.1979(11) |
| *b*, Å | 24.976(6) | 25.000(5) | 18.7033(12) |
| *c*, Å | 9.6202(11) | 9.6413(12) | 14.1060(14) |
| α, deg | 90 | 90 | 90 |
| *β*, deg | 91.191(11) | 90.434(11) | 107.276(6) |
| *γ*, deg | 90 | 90 | 90 |
| *V*, Å$^3$ | 4561.4(14) | 4551.2(12) | 3073.0(5) |
| Z | 4 | 4 | 4 |
| $d_{calc,}$ g cm$^{-3}$ | 1.378 | 1.383 | 1.602 |
| temp, K | 293(2) | 293(2) | 293(2) |
| *λ*, Å | 0.710 73 | 0.710 73 | 0.710 73 |
| *μ*, mm$^{-1}$ | 1.069 | 1.131 | 1.745 |
| R1 | 0.0549 | 0.0931 | 0.0490 |
| R2 | 0.1142 | 0.1091 | 0.1229 |

*ν*(C−C) + *ν*(C−N)/pyrazole ring, 1585 m; *ν*(C−C + C−N), 1467 s; $\nu_{as}$(Cl−O), 1112 s; *δ*(O−Cl−O), 632 m. $\mu_{eff}$: 1.86 $\mu_B$ at 25 °C.

**[CuZnL$^m$(*μ*-pz)]BPh$_4$ (3).**[28] To a dry acetonitrile solution (10 mL) of $H_2L^1$ (0.23 g, 0.5 mmol) was added triethylamine (0.5 mmol) and then 1 equiv of $Zn(ClO_4)_2\cdot 6H_2O$ (0.18 g, 0.5 mmol) while stirring under $N_2$. After 15 min, a stoichiometric amount of $[Cu(CH_3CN)_4]ClO_4$ (0.17 g, 0.5 mmol) in acetonitrile (10 mL) was added followed by pyrazole (35 mg, 0.5 mmol). The resulting red-brown solution was exposed to air and stirred further at room temperature for ca. 2 h to get a light brown solution. The complex was isolated as brown crystalline solid by filtering the solution, exchanging anion ($NaBPh_4$ in $CH_3CN$), reducing solvent volume, and recrystallizing ($CH_3CN$). Yield: 0.17 g (36%). Anal. Calcd for $C_{47}H_{51}N_8S_2OCuZnB$: C, 59.59; H, 5.38; N, 11.82. Found: C, 60.06; H, 5.16; N, 11.91. IR (KBr pellet), cm$^{-1}$: *ν*(C−C), 1579 s; *ν*(C−N)/pyrazole ring, 1553 m; *ν*(C−C + C−N), 1473 s; *ν*($BPh_4^-$), 735 and 707 s. $\mu_{eff}$: 1.88 $\mu_B$ at 25 °C.

**[CuZnL$^2$(*μ*-pz)]ClO$_4\cdot$CH$_3$CN (4).** This compound was prepared by following a similar procedure as described for **3** using $H_2L^2$ as the ligand instead of $H_2L^1$, and the complex was isolated as perchlorate salt. Yield: 0.19 g (56%). Anal. Calcd for $C_{23}H_{30}N_9S_2O_5$-CuZnCl: C, 37.28; H, 4.05; N, 17.02. Found: C, 37.26; H, 3.93; N, 16.85. IR (KBr pellet), cm$^{-1}$: *ν*(C−C) + *ν*(C−N)/pyrazole ring, 1583 s; *ν*(C−C + C−N), 1475 s; $\nu_{as}$(Cl−O), 1094 s; *δ*(O−Cl−O), 624 s. $\mu_{eff}$: 1.86 $\mu_B$ at 25 °C.

**Caution!** *Perchlorate salts of metal complexes containing organic ligands are potentially explosive*[29] *and should be handled in small quantity with sufficient care.*

**Physical Measurements.** Elemental analyses (C, H, and N), IR, and UV−vis spectra were obtained as described elsewhere.[30,31] Mass spectroscopy was performed on a LCQ Finnigan electrospray ionization mass spectrometer with electrospray ionization (ESI) source. Magnetic moments of the powdered polycrystalline samples at room temperature were calculated from the data obtained on a PAR 155 vibrating-sample magnetometer. Variable-temperature magnetic susceptibility data and magnetization measurements on powdered samples of complexes **1** and **2** were performed on a Cryogenics S600 SQUID magnetometer in the temperature range 4−300 K with an applied field of 0.1 T. A diamagnetic correction, estimated from Pascal's constants, was applied on the experimental susceptibilities to give molar paramagnetic susceptibilities. The ESR spectra of the powder samples were recorded on a Varian E-9 spectrometer working at X-band (9.25 GHz) which was equipped with an Oxford Instruments ESR9 helium flux cryostat to work at temperatures between room temperature and 4 K. ESR spectra in solution were taken on a JEOL JES-RE3X X-band spectrometer, equipped with a standard low-temperature apparatus and data processing system ESPRIT 330. Cyclic voltammetry in dry acetonitrile solution was performed with a BAS model 100B/W electrochemical work station using platinum disk working (i.d. = 1.6 mm at $\upsilon < 1$ V s$^{-1}$ and i.d. = 10 $\mu$m at $\upsilon > 1$ V s$^{-1}$) and platinum wire counter electrodes. Ag/AgCl electrode (3 M NaCl) was used for reference, and ferrocene as internal standard.[32] Solutions were ∼1.0 mM in samples and contain 0.1 M tetrabutylammonium perchlorate (TBAP) as the supporting electrolyte. Bulk electrolysis was carried out using a platinum-gauze working electrode.

**X-ray Crystallography.** Diffraction quality crystals of **1** (dark brown rectangular rod, 0.43 × 0.20 × 0.17 mm), **3** (red block, 0.34 × 0.33 × 0.20 mm), and **4** (yellow cylinder, 0.30 × 0.30 × 0.30 mm) were grown at room temperature by slow evaporation of the acetonitrile solutions of the compounds. Intensity data for the compounds were measured on an Enraf-Nonius CAD-4 diffractometer using graphite-monochromated Mo Kα ($\lambda$ = 0.710 73 Å) radiation in the $\omega-2\theta$ scan mode. Accurate cell parameters and an orientation matrix were determined by least-squares fit of 25 centered reflections. The intensity data were corrected for empirical absorption. The structures were solved by direct methods[33] and refined on $F^2$ by a full-matrix least squares procedure[34] with anisotropic displacement parameters for the non-hydrogen atoms, based on all data minimizing $R2 = [\Sigma[w(F_o^2 - F_c^2)^2]/\Sigma[(F_o^2)^2]]^{1/2}$, $R1 = \Sigma||F_o| - |F_c||/\Sigma|F_o|$, and $S = [\Sigma[w(F_o^2 - F_c^2)^2]/(n - p)]^{1/2}$. Hydrogen atoms were placed in the calculated positions with isotropic displacement parameters. Crystal parameters and the details of the data collections and refinement are summarized in Table 1. The perchlorate anion is disordered over four sites in complex **4**.

## Results and Discussion

**Syntheses.** The protocol used for the syntheses of the compounds **1**−**4** is displayed in Scheme 1. The dicopper(II)

(29) Wolsey, W. C. *J. Chem. Educ*. **1973**, *50*, A335.
(30) Dutta, S. K.; Kumar, S. B.; Bhattacharyya, S.; Tiekink, E. R. T.; Chaudhury, M. *Inorg. Chem*. **1997**, *36*, 4954.
(31) Dutta, S. K.; McConville, D. B.; Youngs, W. J. *Inorg. Chem*. **1997**, *36*, 2517.
(32) Gagné, R. R.; Koval, C. A.; Lisensky, G. C. *Inorg. Chem*. **1980**, *19*, 2854.
(33) Sheldrick, G. M. SHELXS 97. *Acta Crystallogr*. **1990**, *A46*, 467.
(34) Sheldrick, G. M. *SHELXL-97. Release 97-1, Program for the Refinement of Crystal Structures*; University of Göttingen: Göttingen, Germany, 1997.

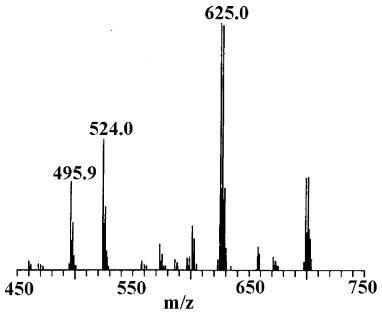


**Figure 1.** ESI mass spectrum of **1**.

**Scheme 1**

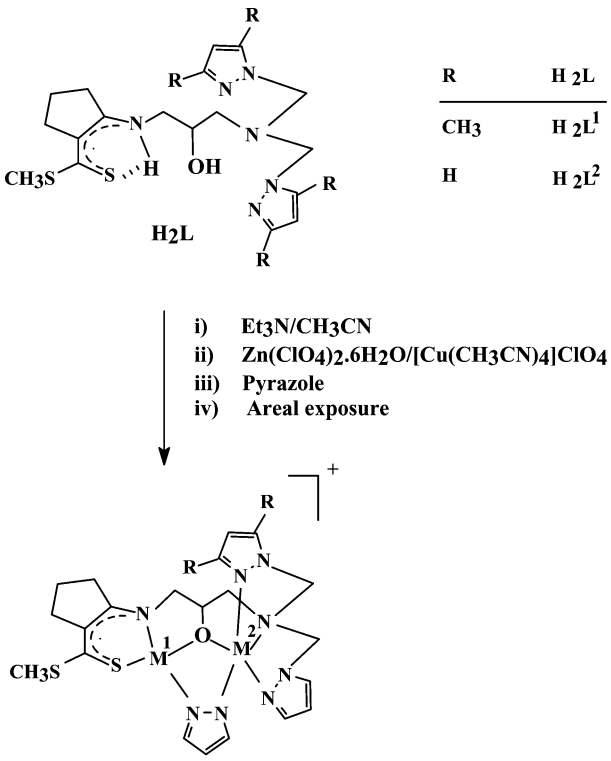


**1** $M^1 = M^2 = Cu(II)$; R = $CH_3$
**2** $M^1 = M^2 = Cu(II)$; R = H
**3** $M^1 = Cu(II)$, $M^2 = Zn(II)$; R = $CH_3$
**4** $M^1 = Cu(II)$, $M^2 = Zn(II)$; R = H

complexes **1** and **2** of the dinucleating ligands $H_2L^1$ and $H_2L^2$, respectively, have been obtained in moderate yields by the reaction of $[Cu^I(CH_3CN)_4]ClO_4$ with stoichiometric amounts of the ligands (2:1 mol ratio) in acetonitrile in the presence of added base and the bridging pyrazole ligand and subsequent exposure to atmospheric oxygen. During the reaction, $H_2L^1$ undergoes an interesting change when dimethylpyrazole from one of its pyrazolyl arms gets exchanged with an extraneous pyrazole molecule, the latter being added to bridge the metal centers as confirmed by mass spectral (Figure 1) and crystal structure analysis (see later). The presence of bulky anion, e.g. $BPh_4^-$, is needed to induce crystallization of **1**. Our initial attempts to prepare these compounds using copper(II) salts as the metal ion precursor were unsuccessful because of the reducing nature of cyclopentenedithiocarboxylate-based ligands,[23] leading to intractable solid(s) of unknown composition. To prevent such undesirable reductions from happening, $[Cu(CH_3CN)_4]ClO_4$ was used as the metal ion precursor.

The pyrazolate-bridged Cu/Zn compounds **3** and **4** are conveniently prepared by a single-pot synthesis in acetonitrile through sequential addition of equimolar amounts of $Zn(ClO_4)_2 \cdot 6H_2O$ and $[Cu^I(CH_3CN)_4]ClO_4$ to a stoichiometric amount of the dinucleating ligand in the presence of added base and the bridging pyrazole ligand and their subsequent exposure to atmospheric oxygen. Reversal of the sequence of metal ion addition does not however affect the course of this reaction. The interesting aspect of this preparative procedure is the regioselective nature of these asymmetric binucleating ligands which can selectively bind copper(I) in one of the sites that involves the ONS donor set, thus offering an opportunity to isolate a heterobinuclear compound by a single step reaction. All the imidazole-bridged Cu/Zn acyclic binuclear complexes reported thus far[11−17] have been prepared by combining the preformed mononuclear Cu(II) and Zn(II) parts, baring a single incidence,[16] where single-pot synthesis by sequential addition of the metal ions has been successfully carried out. Compound **3** (as compound **1)** has the ligand $H_2L^1$ in the modified form $[L^m]^{2-}$ and needs a bulky anion for its crystallization. The steric constraints imposed by the dimethylpyrazolyl arms of the ligand $H_2L^1$ could be the driving force for such exchange reaction. This explanation gains further ground by the isolation of a compound with ligand structure of $H_2L^1$ remaining intact when a larger cation, viz. $Cd^{2+}$, is used to replace $Zn^{2+}$ ion in **3**.[35] Use of imidazole as a bridging ligand in the above syntheses did not yield the desired products.

IR spectra of the complexes contain all the pertinent bands of the coordinated asymmetric ligands. Two such prominent bands appearing at ca. 1550 and 1470 $cm^{-1}$ regions are due to stretching modes, associated with the pyrazole and cyclopentene rings, respectively. In addition, both complexes **2** and **4** display a couple of strong bands at 1100 and 630 $cm^{-1}$, confirming the presence of ionic perchlorate.[36]

**Description of Crystal Structures.** ORTEP views of the binuclear complexes **1**, **3**, and **4** are shown in Figures 2−4, respectively. Selected bond distances and angles are summarized in Table 2. The ligand in complexes **1** and **3** has a modified structure $[L^m]^{2-}$ involving the replacement of dimethylpyrazolyl part by pyrazole in one of the appended arms as confirmed by X-ray crystallography (Figures 2 and 3). All the three complexes crystallize in monoclinic space group $P2_1/n$ ($P2_1/c$ for **4**; Figure 4) with four molecular weight units/cell.

In the dicopper complex **1**, one of the metal centers Cu(1) has an approximate square-planar geometry. The bridging alkoxy atom O(1) and N(3) and S(2) from the tridentate part of the ligand, together with N(2) from the bridging pyrazolyl moiety, define this plane and lie −0.0641, 0.0476, −0.0468, and 0.0481 Å, respectively, out of the least-squares plane through them. The Cu(1) atom is displaced

(35) Ghosh, D.; Tiekink, E. R. T.; Caneschi, A.; Chaudhury, M. Unpublished work.
(36) Nakamoto, K. *Infrared and Raman Spectra of Inorganic and Coordination Compounds*, 3rd ed.; Wiley-Interscience: New York, 1978.

**Table 2.** Selected Bond Distances (Å) and Angles (deg)[a] for Complexes **1**, **3**, and **4**

| | 1 | 3 | 4 |
|---|---|---|---|
| M(1)····M(2) | 3.3687 | 3.3782 | 3.3403 |
| M(1)−O(1) | 1.893(6) | 1.921(6) | 1.910(3) |
| M(1)−N(3) | 1.904(10) | 1.946(7) | 1.960(4) |
| M(1)−N(2) | 1.938(10) | 1.990(8) | 1.991(4) |
| M(1)−S(2) | 2.226(2) | 2.228(3) | 2.2275(15) |
| M(2)−O(1) | 1.890(8) | 1.929(6) | 1.927(3) |
| M(2)−N(1) | 1.974(8) | 1.991(8) | 1.977(4) |
| M(2)−N(8) | 2.022(12) | 2.042(9) | 2.027(4) |
| M(2)−N(6) | 2.113(8) | 2.445(8) | 2.427(4) |
| M(2)−N(4) | 2.161(7) | 2.012(9) | 2.012(4) |
| C(2)−S(2) | 1.746(12) | 1.726(11) | 1.720(5) |
| O(1)−M(1)−N(3) | 84.4(4) | 84.3(3) | 83.50(15) |
| O(1)−M(1)−N(2) | 84.9(4) | 87.3(3) | 88.65(15) |
| N(3)−M(1)−N(2) | 169.0(3) | 171.2(4) | 172.03(17) |
| O(1)−M(1)−S(2) | 175.7(3) | 176.3(2) | 179.28(12) |
| N(3)−M(1)−S(2) | 97.2(2) | 96.6(3) | 96.91(13) |
| N(2)−M(1)−S(2) | 93.6(2) | 91.9(3) | 90.93(12) |
| O(1)−M(2)−N(1) | 87.2(4) | 89.4(3) | 90.45(15) |
| O(1)−M(2)−N(8) | 136.6(4) | 121.0(3) | 111.03(17) |
| N(1)−M(2)−N(8) | 105.7(4) | 109.3(4) | 109.23(18) |
| O(1)−M(2)−N(6) | 83.2(4) | 76.6(3) | 76.98(14) |
| N(1)−M(2)−N(6) | 170.0(3) | 165.3(3) | 167.43(15) |
| N(8)−M(2)−N(6) | 79.7(4) | 74.9(4) | 76.28(16) |
| O(1)−M(2)−N(4) | 110.1(4) | 112.8(3) | 123.19(17) |
| N(1)−M(2)−N(4) | 105.3(3) | 113.4(4) | 112.04(18) |
| N(8)−M(2)−N(4) | 106.1(3) | 109.6(4) | 109.14(17) |
| N(6)−M(2)−N(4) | 80.6(3) | 77.1(4) | 75.44(16) |
| M(1)−O(1)−M(2) | 125.9(6) | 122.7(4) | 121.04(16) |

[a] M(1) = Cu(1), M(2) = Cu(2) in **1** and M(1) = Cu, M(2) = Zn in **3** and **4**.

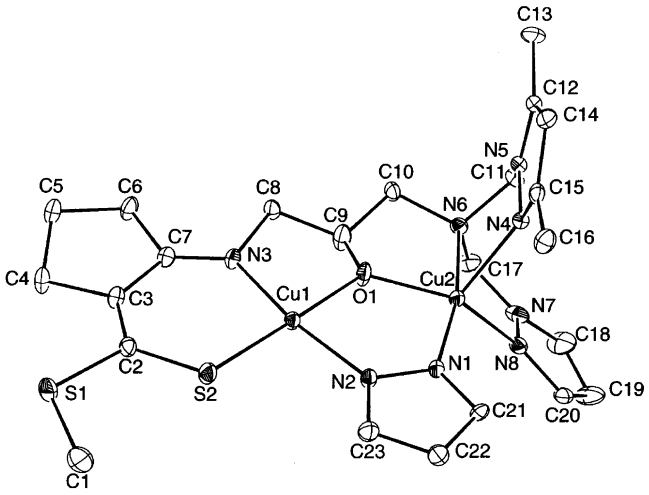


**Figure 2.** ORTEP drawing and crystallographic numbering scheme for complex **1**.

by 0.0152 Å out of this plane. The trans angles N(3)−Cu(1)−N(2) 169.0(3)° and S(2)−Cu(1)−O(1) 175.7(3)° are close to linearity. The adjacent metal center Cu(2) on the other hand is five-coordinate with a highly distorted square-pyramidal geometry as indicated by the structural indexing parameter $\tau$ which measures the degree of trigonality of pentacoordination geometry between an ideal square-pyramidal ($\tau = 0$) and a trigonal-bipyramidal ($\tau = 1$) extremes.[37] For the Cu(2) center in **1**, $\tau = 0.54$ and its distorted basal plane is defined by the O(1), N(6), and N(8)

(37) Addison, A. W.; Rao, T. N.; Reedijk, J.; Rijin, J.; Verschoor, G. C. *J. Chem. Soc., Dalton Trans.* **1984**, 1349. (b) Cornman, C. R.; Geiser-Bush, K.; Rowtey, S. P.; Boyle, P. D. *Inorg. Chem.* **1997**, *36*, 6401.

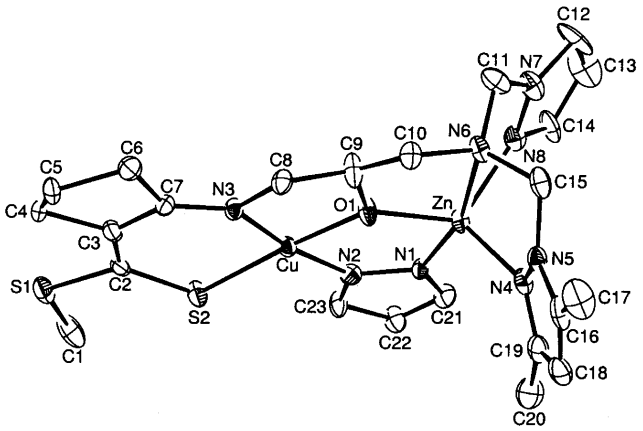


**Figure 3.** ORTEP drawing and crystallographic numbering scheme for complex **3**.

atoms, derived from the tetracoordinating part of the asymmetric ligand, and N(1) atom of pyrazole, the bridging ancillary ligand. The apical position is occupied by the remaining pyrazolyl nitrogen atom N(4). The deviations from the least-squares plane through the O(1), N(6), N(8), and N(1) atoms comprising the square plane are 0.3131, −0.3074, 0.2520, and −0.2578 Å, respectively. The trans angle O(1)−Cu(2)−N(8) (136.6(4)°) is very short of linearity, all these giving indications of extreme distortion in the basal plane. The Cu(2) atom is shifted by 0.3893 Å out of this plane toward the apical nitrogen atom N(4). The copper(II) centers are almost equidistant from the bridging alkoxy atom O(1) (Cu(1)−O(1), 1.893(6) Å, and Cu(2)−O(1), 1.890(8) Å) as are the Cu−N distances Cu(1)−N(2) (1.938(10) Å) and Cu(2)−N(1) (1.974(8) Å) from the bridging pyrazolyl nitrogens. The Cu(1)···Cu(2) separation (3.3687 Å) is much shorter than the corresponding distance (6.097 Å) in the imidazole-bridged dicopper system.[17b] The Cu(1)−O(1)−Cu(2) bridge angle is 125.9(6)°.

The copper(II)−zinc(II) heterodinuclear complexes **3** and **4** have essentially similar structures with almost identical metrical parameters (Table 2). The copper(II) sites in these complexes have square-planar geometry comprising the S(2), N(3), O(1), and N(2) atoms, similar to what is observed for the Cu(1) site in the dicopper complex **1** and lie −0.0450 (−0.0059 for **4**), 0.0529 (0.0069), −0.0602 (−0.0078), and 0.0523 Å (0.0068 Å), respectively, out of the least-squares plane through these atoms. The Cu atom is displaced by 0.0125 Å (0.0176 Å) out of this plane. The trans angles N(3)−Cu−N(2), 171.2(4) (172.03(17)°), and O(1)−Cu−S(2), 176.3(2) (179.28(12)°), are close to linearity, as expected for a regular square-planar geometry. The Zn sites have distorted trigonal-bipyramidal geometry with $\tau = 0.74$ (0.73). The basal plane is comprised of the bridging alkoxy atom O(1) and the pyrazolyl nitrogen atoms N(8) and N(4), all from the tetradentate part of the asymmetric ligand. The apical positions are occupied by the tertiary amino nitrogen N(6) and the bridging pyrazolyl nitrogen atom N(1). The distances of the metal centers from the bridging alkoxy atom Cu−O(1), 1.921(6) Å (1.910(3) Å), and Zn−O(1), 1.929(6)Å (1.927(3) Å), are almost identical as are the distances from bridging pyrazolyl nitrogens Cu−N(2),

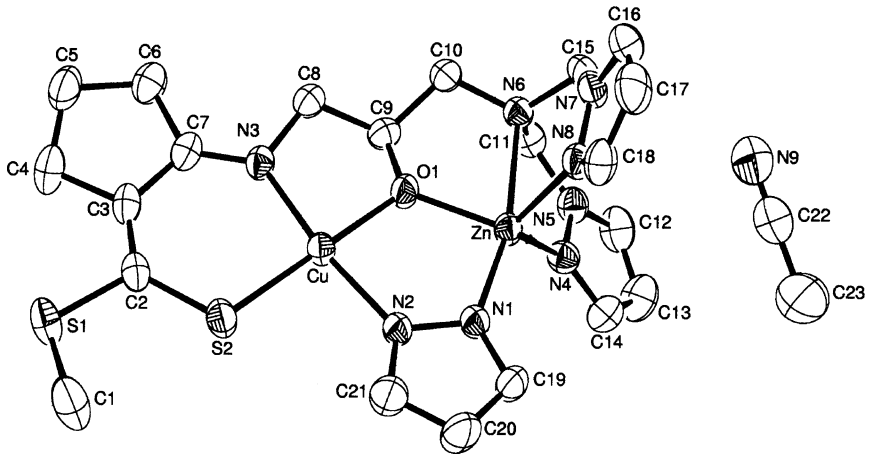


**Figure 4.** ORTEP drawing and crystallographic numbering scheme for complex **4**.

1.990(8) Å (1.991(4) Å), and Zn−N(1), 1.991(8) Å (1.977(4) Å). The bridge angle Cu−O(1)−Zn is 122.7(4)° (121.04(16)°), and the separation between the metal centers Cu···Zn is 3.3782 Å (3.3403 Å); both of these are almost identical with the corresponding values for the dicopper compound **1**.

A closer look in Table 2, however, reveals some interesting points. All the bond lengths except Cu(1)−S(2) around the Cu(1) site in **1** are shorter than the corresponding bond distances around the Cu sites in **3** and **4**. This expansion in copper coordination geometry in the latter compounds is possibly due to the influence of the adjacent metal center. In **1**, this center is occupied by another Cu(II) ion having a distorted square-pyramidal geometry with axially elongated (Cu(2)−N(4), 2.161(7) Å) structure, not uncommon for a Jahn−Teller ion. In **3** and **4** on the other hand, the site is occupied by a Zn(II) ion with highly distorted TBP geometry as revealed from the elongated Zn−N(6) distance, 2.445(8) Å (2.427(4) Å). This change over in coordination geometry probably generates sufficient strain in the remaining part of the ligand molecule, and this in turn is released by the expansion of the relevant bond distances.

**Magnetic Properties of Cu(II)−Cu(II) Homodinuclear Complexes**. Variable-temperature susceptibility measurements were carried out for the dicopper(II) complexes **1** in the temperature range 300−50 K and for **2** in the range 300−4 K. The $\chi_M$ versus $T$ plots are shown in Figure 5. It may be noted that, for both compounds **1** and **2**, the susceptibility values increase monotonically between 50 and 200 K with the rise of temperature and thereafter increase slowly to provide maxima at ca. 260 K. The observed behavior is clearly indicative of the presence of strong antiferromagnetic exchange interaction between the two copper(II) centers in these compounds. In the case of **2**, on further lowering of temperature the $\chi_M$ value begins to increase rapidly below 30 K. The observed behavior is due to the presence of small amount of mononuclear copper(II) impurity, a phenomenon common for this type of compound.[16,17] The susceptibility data for both compounds were fitted to the modified form of Bleany−Bowers equation for

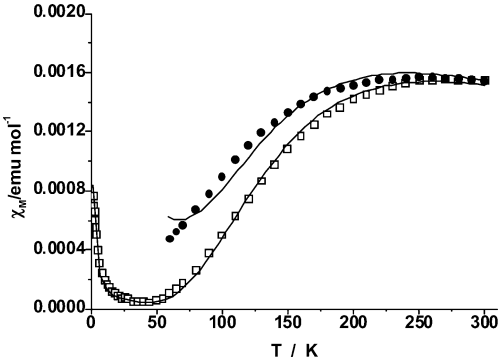


**Figure 5.** Temperature dependence of the molar magnetic susceptibility ($\chi_M$) for **1** (full circles) and **2** (empty squares). The solid lines result from least-squares fits according to the modified Bleaney−Bowers eq 3. Best fit parameters are reported in the text.

exchange-coupled pairs of copper(II) ions (eq 3),[38] which includes the term $\rho$ for the mole fraction of the mononuclear copper(II) impurity. In eq 3, $J$ is the spin-exchange coupling constant in the spin Hamiltonian $H = -JS_1S_2$, while the other terms have their usual significance. The best fit curves (shown as solid line in Figure 5) obtained from nonlinear least-squares analysis of $\chi_M - T$ data give $J = -285 \pm 5$ cm$^{-1}$, $g = 2.05 \pm .02$, $\rho = (3.8 \pm 0.05) \times 10^{-2}$, and $R^2 = 3.7 \times 10^{-4}$ for **1** and $-296 \pm 3$ cm$^{-1}$, $2.07 \pm .02$, $(1.85 \pm 0.1) \times 10^{-3}$, and $1.9 \times 10^{-4}$, respectively, for **2**. The results indicate strong antiferromagnetic interactions in compounds **1** and **2** as observed in several other reported complexes ($-J = 100-300$ cm$^{-1}$) with similar $\mu$-alkoxo $\mu$-pyrazolato doubly bridged structures.[39−41]

$$\chi = \frac{2N_A g^2 \mu_B{}^2}{kT}[3 + \exp(-J/kT)]^{-1}(1-\rho) + \rho\frac{N_A g^2 \mu_B{}^2}{2kT} \quad (3)$$

The $J$ values for **1** and **2** are significantly larger in comparison to imidazolate-bridged dicopper(II) complexes for which the $J$ values lie in the range 0−160 cm$^{-1}$.[16,17,42] It

(38) Bleaney, B.; Bowers, K. D. *Proc. R. Soc. London, A* **1952**, *214*, 451.
(39) Doman, T. N.; Williams, D. E.; Banks, J. F.; Buchanan, R. M.; Chang, H.; Webb, R. J.; Hendrickson, D. N. *Inorg. Chem.* **1990**, *29*, 1058.
(40) Nishida, Y.; Kida, S. *Inorg. Chem.* **1988**, *27*, 447.
(41) Mazurek, W.; Kennedy, B. J.; Murray, K. S.; O'Connor, M. J.; Rodgers, J. R.; Snow, M. R.; Wedd, A. G.; Zwack, P. R. *Inorg. Chem.* **1985**, *24*, 3258.

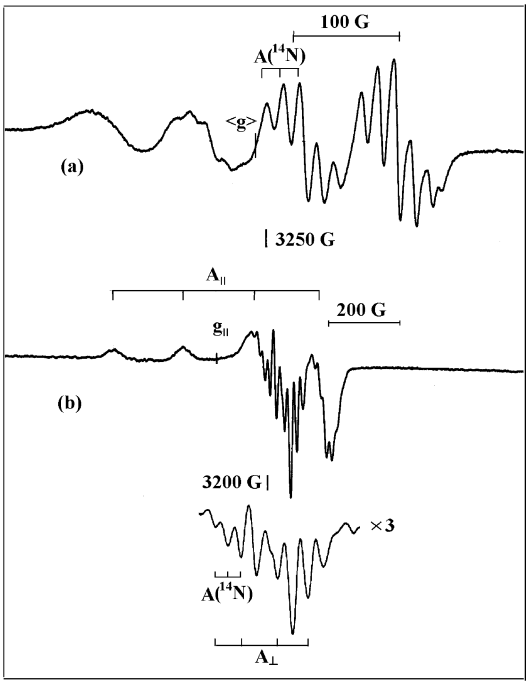


**Figure 6.** EPR spectra of **4** in $CH_3CN$/toluene (1:3 v/v) solution at (a) 298 K and (b) 77 K.

**Table 3.** EPR Data for Complexes **3** and **4**

| complex | $\langle g\rangle^a$ | $10^4\langle A\rangle^a/cm^{-1}$ | $g_{\|}{}^b$ | $g_{\perp}{}^b$ | $10^4A_{\|}{}^b$ | $10^4A_{\perp}{}^b$ | $10^4A(^{14}N)^a$ |
|---|---|---|---|---|---|---|---|
| **3** | 2.085 | 88 | 2.152 | 2.043<br>2.051[c] | 198 | 31.3<br>32[c] | 15.3 |
| **4** | 2.085 | 88 | 2.154 | 2.046<br>2.050[c] | 202 | 33.1<br>31[c] | 15.5 |

[a] From room-temperature spectra in acetonitrile/toluene (1:3 v/v) solution. [b] From frozen solution (77 K) spectra. [c] Calculated from the equation $\langle g\rangle = {}^1/_3[g_{\|} + 2g_{\perp}]$ and $\langle A\rangle = {}^1/_3[A_{\|} + 2A_{\perp}]$.

thus appears that bridged pyrazolate offers a more efficient pathway for the interaction of the odd electrons of the dicopper(II) systems compared to what is observed in the related imidazolate-bridged compounds. A more probable reason for this is the Cu(II)−Cu(II) distance which is significantly shorter (ca 3.35 Å) in the $\mu$-pyrazolate complexes than in the $\mu$-imidazolate type (ca 6.10 Å).[16,17] Bridging ligands thus play a crucial role in modulating the $J$ value which decreases in the order $OR^-$ ≈ pyrazolate > acetate ≈ $OH^-$ > $Cl^-$ for a group of related dicopper(II) complexes with varying bridging ligands.[41]

**EPR Spectroscopy.** The dicopper complexes **1** and **2** are EPR silent at room temperature and at 77 K both in solution ($CH_3CN$/toluene, 1:3 v/v) and in the solid state due to their strong antiferromagnetic coupling which is still active in this temperature range as revealed from magnetic measurements (vide supra).

Spectra of the Cu(II)−Zn(II) complexes **3** and **4** are almost identical and show the usual features of a mononuclear Cu(II) center. A set of spectra for compound **4** is displayed in Figure 6 as a representative, and the data are summarized in Table 3. The room-temperature spectrum (Figure 6a) shows typical four-line ($^{63,65}$Cu; $I = {}^3/_2$) feature with each

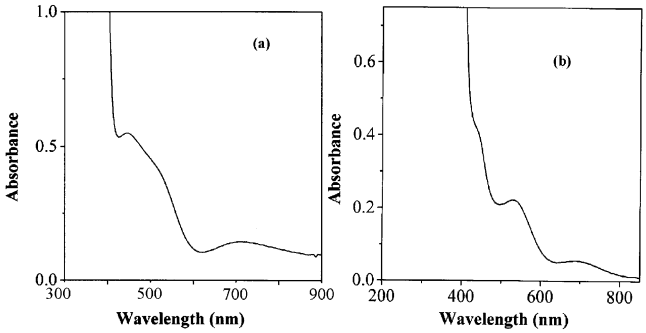


**Figure 7.** Electronic absorption spectra of **1** (frame a) and **3** (frame b) in acetonitrile.

**Table 4.** Summary of Electronic Spectral Data for Complexes **1**−**4** in $CH_3CN$

| complex | $\lambda_{max}$/nm ($\epsilon_{max}$/mol$^{-1}$ cm$^2$) |
|---|---|
| **1** | 708 (280), 516 (sh), 444 (1100), 384 (11 300), 330 (16 100), 288 (14 400) |
| **2** | 687 (270), 520 (sh), 441 (990), 381 (10 200), 328 (14 400), 288 (12 700) |
| **3** | 680 (60), 533 (230), 439 (sh), 383 (11 200), 326 (15 100), 288 (13 300) |
| **4** | 695 (50), 535 (210), 437 (sh), 382 (10 400), 328 (13 900), 288 (12 700) |

stronger line being split into three components by strong nitrogen ($^{14}$N; $I = 1$) superhyperfine couplings ($A_N = 15.3 \times 10^{-4}$ cm$^{-1}$). This is even reflected in the frozen solution (77 K) spectrum (Figure 6b) which reveals an axially symmetric anisotropy with $g_{\perp}$ region showing multiple N-superhyperfine lines. Such a spectrum is seldom observed for N-coordinated Cu(II) complexes and strongly suggests a large amount of electronic delocalization through the bridging pyrazolate ligand. The observed trend in the spin-Hamiltonian parameters ($g_{\|} > g_{\perp} > 2.04$ and $|A_{\perp}| \ll |A_{\|}| \approx (120-150) \times 10^{-4}$ cm$^{-1}$) indicates a $d_{x^2-y^2}$-based ground state with tetragonal site symmetry for Cu(II) in the complexes **3** and **4** as expected from structural and ligand features.[43]

**Electronic Spectroscopy.** Electronic spectra of the complexes **1**−**4** have been recorded in acetonitrile, and the data are summarized in Table 4. A representative spectrum for each type of compound (**1** and **3**) is displayed in Figure 7, which reveals their close similarity. In the visible region, each of these spectra involves two ligand-field bands, appearing at 708−680 nm and 535−516 nm regions, corresponding to the transitions $d_{z^2} \rightarrow d_{x^2-y^2}$ and $d_{xz}$, $d_{yz} \rightarrow d_{x^2-y^2}$, respectively, as expected for square-planar Cu(II) complexes and confirming the $d_{x^2-y^2}$-based ground state.[43,44] The latter band for the complexes **1** and **2** appears in the form of a broad shoulder with increased intensity (Figure 7a), gained from the contribution of the only d−d band due to the second Cu(II) center of distorted square-pyramidal geometry.[45,46] The compounds also show two strong bands

(42) Strotkamp, K. G.; Lippard, S. J. *Acc. Chem. Res.* **1982**, *15*, 318.
(43) Hathaway, B. J.; Billing, D. E. *Coord. Chem. Rev.* **1970**, *5*, 143.
(44) Lever, A. B. P. *Inorganic Electronic Spectroscopy*, 2nd ed.; Elsevier: New York, 1984.
(45) McLachlan, G. A.; Fallon, G. D.; Martin, R. L.; Spiccia, L. *Inorg. Chem.* **1995**, *34*, 254.
(46) Hathaway, B. J. In *Comprehensive Coordination Chemistry*; Wilkinson, G., Gillard, R. D., McCleverty, J. A., Eds.; Pergamon Press: Oxford, England, 1987; Vol. 5, p 533.

**Table 5.** Summary of Electrochemical Data[a]

| complex | process I $E_{1/2}$[b]/V | process II $E_{pc}$[b]/V | process III $E_{pa}$[b]/V |
|---|---|---|---|
| **1** | −0.26 | −1.35 | 0.96 |
| **2** | −0.26[c] | −1.42 | 1.00 |
| **3** | | −1.01 | 0.89 |
| **4** | | −0.93 | 0.91 |

[a] Solvent: acetonitrile. Supporting electrolyte: TBAP (0.1 M). Solute concentration: ca. $10^{-3}$ M. Working electrode: platinum. Temperature: 25 °C. [b] Potentials are vs Ag/AgCl (3 M NaCl) and estimated by cyclic voltammetry at a scan rate of 100 mV $s^{-1}$. $E_{1/2} = 0.5(E_{pc} + E_{pa})$. [c] The value represents the irreversible peak potential.

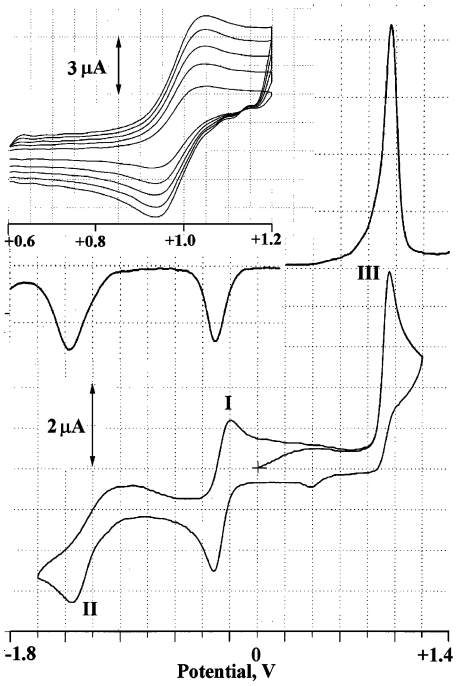


**Figure 8.** Top: Differential pulse voltammogram of **1** at −5 °C using a scan rate of 20 mV $s^{-1}$ in $CH_3CN$. The pulse amplitude is 50 mV. Bottom: Cyclic voltammogram of **1** in acetonitrile at a platinum electrode with scan rate 100 mV $s^{-1}$ and temperature 25 °C. The inset shows voltammograms for the oxidation process (process III) at $\upsilon = 50$, 40, 30, 20, and 10 V $s^{-1}$.

in the near-UV region at ca. 440 and 380 nm of which the former appears as a shoulder in **3** and **4** and is tentatively assigned due to $\mu$-pyz → Cu(II) charge transfer. The remaining one with strong intensity ($\epsilon$, 10 200−11 300 $mol^{-1}$ $cm^2$), we suggest, is originating from S($\pi$) → Cu(II) charge transfer on the basis of analogy to similar reported complexes.[47] The remaining bands at still higher energies are due to ligand-internal transitions.

**Electrochemistry.** The redox properties of the complexes are summarized in Table 5, and the cyclic voltammogram of the dicopper complex **1** is displayed in Figure 8. It involves a quasireversible reduction process (process I) at $E_{1/2} = -0.26$ V ($\Delta E_p$, 122 mV; $i_{pc}/i_{pa}$, 1.1), followed by an irreversible reduction (process II) at $E_{pc} = -1.35$ V vs Ag/AgCl reference, both involving an identical number of electron(s) as revealed from DPV experiments, also shown in Figure 8. Comparison with ferrocenium/ferrocene couple as an internal standard[32] ($\Delta E_p$, 80 mV; $i_{pc}/i_{pa}$, 1.0 at 100 mV $s^{-1}$) gives an indication of monoelectronic nature of these couples. In the anodic range, an irreversible oxidation (process III) is observed at $E_{pa} = 0.96$ V. The oxidized species is not stable enough to appear in the reverse scan of 100 mV $s^{-1}$. At a very high scan rate ($\upsilon >$ 1000 mV $s^{-1}$), however, the oxidized species does survive to appear as a quasireversible voltammogram as shown in Figure 8, inset ($E_{1/2} = 0.99$ V, $\Delta E_p = 106$ mV). The electron stoichiometry appears to be twice as high as that of the other two processes as indicated by the current height from DPV study. The remaining dicopper compound **2** displays an almost similar voltammogram (Table 5) excepting process I which appears to be an irreversible process in the latter case but appearing in the same region at $E_{pc} = -0.26$ V.

The Cu(II)−Zn(II) complexes on the other hand show two irreversible processes, one each in the cathodic and anodic regions at −1.01 V (−0.93 V for **4**) and 0.89 V (0.91 V), respectively, which show an overall similarity with the electrochemical processes II and III, respectively, of the dicopper(II) system. The results are in agreement with the presence of only one copper(II) site in **3** and **4**. A comparison of the electrochemical potentials in Table 5 thus indicates that the process I in **1** and **2** is due to a one-electron [Cu(II)−Cu(II)/Cu(II)−Cu(I)] reduction involving the square-pyramidal copper site, while the reduction [Cu(II)−Cu(I)/Cu(I)−Cu(I)] at more negative potential (process II) involves the square-planar copper center. The oxidation process (process III) for **1** and **2** on the other hand possibly involves a couple of electrons (as judged from the DPV current height), resulting in a single-step two-electron transfer. Coulometric confirmation of this is however not possible due to the instability of these compounds in the required longer time scale. We are thus not quite sure at this stage whether this oxidation is a metal-based [Cu(II)−Cu(II)/Cu(III)−Cu(III)] process or a ligand-based one. Electrochemical response(s) of the corresponding dizinc compound could have been helpful to choose between the alternatives. Unfortunately, we are unable to synthesize the dizinc compound.

## Concluding Remarks

The work presented in this report is centered around the syntheses of a pair of heterobinuclear Cu(II)−Zn(II) compounds **3** and **4** and their dicopper(II) counterparts **1** and **2** using the binucleating ligands $H_2L^1$ and $H_2L^2$, capable of providing both donor set and coordination number asymmetry in tandem. Unlike the dinickel compounds described in a previous report,[19] the coordinated $(L^1)^{2-}$ ligand in compounds **1** and **3** undergoes an interesting exchange reaction, possibly driven by a steric factor, when 3,5-dimethylpyrazole from one of its flexible arms gets exchanged with an extraneous pyrazole molecule, added as a bridge between the metal centers. To our knowledge, **3** and **4** are the first examples of heterobinuclear Cu(II)−Zn(II) complexes in asymmetric ligand environment[16,48] and serve as a rudimentary structural model for the Cu−Zn active site

(47) Hughey, J. L., IV; Fawcett, T. G.; Rudich, S. M.; Lalancette, R. A.; Potenza, J. A.; Schugar, H. J. *J. Am. Chem. Soc.* **1979**, *101*, 2617.

(48) Abe, K.; Matsufuji, K.; Ohba, M.; Ōkawa, H. *Inorg. Chem.* **2002**, *41*, 4461.

of bovine erythrocyte SOD.[7,8,18] The pentacoordinated Zn sites in **3** and **4** have distorted TBP geometry ($\tau = 0.74$),[37] while the corresponding Cu site in **1** has a highly distorted square pyramidal ($\tau = 0.54$) structure. The Cu−O(1)−Zn bridge angle (122.7(4)°) and the Cu···Zn separation (3.3403 Å) are close to the corresponding values obtained with the dicopper(II) analogue (**1**) in which the two Cu(II) centers are coupled by strong antiferromagnetic interactions ($J = -290$ cm$^{-1}$). The bridging pyrazolate molecule possibly offer a convenient exchange pathway for this strong antiferromagnetic coupling as revealed from the EPR spectra of the corresponding Cu(II)−Zn(II) complexes. The latter show sizable N-superhyperfine coupling ($A(^{14}\text{N}) = 15.3 \times 10^{-4}$ cm$^{-1}$) in their EPR spectra even at room temperature, thus confirming the mobility of the odd electrons through the pyrazolate bridge.

**Acknowledgment.** This work was supported by the Council of Scientific and Industrial Research (CSIR), New Delhi. D.G., N.K. and G.M. also thank the CSIR for the award of research fellowships. We thank Professor K. Nag and Dr. Rakesh Ganguly for helpful discussions.

**Supporting Information Available:** X-ray crystallographic files in CIF format for compounds **1**, **3**, and **4**. This material is available free of charge via the Internet at http://pubs.acs.org.

IC049449+